Stability analysis of (1+1)-dimensional cnoidal waves in media with cubic nonlinearity

Yaroslav V. Kartashov,[1,2] Victor A. Aleshkevich,[1] Victor A. Vysloukh,[3] Alexey A. Egorov,[1] and Anna S. Zelenina[1]
[1]*Chair of General Physics, Physics Department, M. V. Lomonosov Moscow State University, 119899 Vorobiovy Gory, Moscow, Russia*
[2]*Institute of Photonic Sciences and Department of Signal Theory and Communications, Universitat Politecnica de Catalunya, 08034 Barcelona, Spain*
[3]*Departamento de Fisica y Matematicas, Universidad de las Americas, Puebla, Santa Catarina Martir, Caixa Postal 72820, Puebla, Cholula, Mexico*

(Received 1 July 2002; revised manuscript received 1 November 2002; published 21 March 2003)

In the present paper we perform stability analysis of stationary (1+1)-dimensional cnoidal waves of cn and dn types (anomalous group velocity dispersion) and sn type (normal group velocity dispersion). The mathematical model is based on the nonlinear Schrödinger equation. With this aim we developed a method that takes into consideration the properties of complex eigenvalues of Cauchy matrix for perturbation vectors. We show that cnoidal sn-wave is stable in the whole domain of its existence, whereas cn- and dn-waves are unstable. The instability of cn- and dn-waves is suppressed in the limiting case of strong localization when waves evolve into a set of well-separated fundamental bright solitons.

DOI: 10.1103/PhysRevE.67.036613 PACS number(s): 42.65.Tg, 42.65.Jx, 42.65.Wi

I. INTRODUCTION

The analysis of stability of solitary waves in the frames of various physical models is one of the most interesting and important problems of modern nonlinear optics. Starting from the pioneering paper of Vakhitov and Kolokolov (VK) [1] that was devoted to the derivation of a simple analytical stability criterion (the VK criterion) for (2+1)-dimensional single solitons in focusing saturable media, a number of papers were devoted to the investigation of stability of (1+1)-dimensional multicomponent solitary waves in cubic and saturable media, surface and guided waves, waves in the media with quadratic and competing nonlinearities, etc. The concept of reading of dispersion or Hamiltonian-energy (for Hamiltonian systems) diagrams proved to be especially useful. This concept enables one to make a conclusion about soliton stability directly from dependencies of soliton energy on the propagation constant (or Hamiltonian) without further special analysis [2]. It was shown that the VK stability criterion remains valid in several simplest physical models in (1+1) dimensions, such as models describing surface waves at the interface between a linear dielectric and a cubic medium [3–8], surface waves at the interface between a dielectric and a photorefractive crystal with drift and diffusion nonlinearity [9,10], fundamental soliton states in unidirectional fiber couplers [11,12], birefringent optical fibers [13–16], and type I quadratic solitons [17]. However, for a variety of solitary waves such as multicomponent waves with number of components greater than two [18]; walking vector [19,20]; type II quadratic [21]; walking quadratic [22] solitary waves; dark, gray, and cubic gap solitons [23] the stability criterion can be more complicated than the usual VK criterion or even no evident analytical criterion can exist. Note that papers [2–23] are connected with the investigation of stability of localized (1+1)-dimensional solitary waves.

Recently, a wide class of multicomponent periodical solutions of the (1+1)-dimensional nonlinear Schrödinger equation in the form of cnoidal waves has gained steady attention [24–27]. The concept of periodical solutions of the nonlinear Schrödinger equation is especially attractive from the theoretical point of view because it enables to analyze the propagation dynamics of solitary waves for the cases of different localization of the wave field energy. Cnoidal waves describe periodic arrays of the slit laser beams [28–30], trains of optical pulses in fibers [31–34], and electron wave functions in Bose-Einstein condensates [35,36]. Recently, spatial cnoidal waves were observed experimentally in photorefractive crystals in the steady state regime [30]. One of the most important features of the cnoidal waves is that in the limit of the strong localization they transform into the well-known dark [37] and bright [38] solitons. The latter fact enables to treat cnoidal waves as more general objects than usual localized bright and dark solitons and to analyze the main features of propagation and interaction of pulse trains and beam arrays from the unified point of view.

One of the most interesting problems connected with cnoidal waves is the problem of their stability. Note that upon the analysis of stability of the cnoidal waves one meets serious difficulties connected with nonzero asymptotics of light fields and oscillating character of cnoidal waves. Recently, stability of specific (1+1)-dimensional ''cnoidal waves on a ring'' with respect to stochastic perturbations of input profiles was investigated numerically in Bose-Einstein condensates [35]. At the present moment, stability of cnoidal waves was considered analytically only with respect to a rather narrow class of long-wavelength perturbations [39–43] (the method of stability analysis in approximation of long-wavelength perturbations was first developed in Refs. [44,45]). This approach enables to treat perturbations only with small growth rates (increments), whereas it is commonly known that only perturbations with highest increments survive upon wave propagation [46]. Note also that approaches used in papers [39–42] lead to contradictory conclusions about the stability of cnoidal waves. There is still no self-consistent approach to investigate the stability of (1+1)- and (2+1)-dimensional cnoidal waves for the case of arbitrary perturbation wavelengths.

In the present paper we perform accurate linear stability

analysis of $(1+1)$-dimensional periodical cnoidal waves in optical fibers in the anomalous (waves of cn- and dn-types) and normal (wave of sn-type) dispersion regimes. We developed a method of solution of linearized equation for perturbation vector that is based on the construction of translation matrix for perturbation vector and the analysis of evolution of eigenvalues of this matrix with changes in the parameters of corresponding perturbed cnoidal waves. This approach is semianalytical: computer is used only for multiple calculations of trace of translation matrix. Results of the translation matrix approach are confirmed by direct numerical simulation of perturbed waves propagation. Our approach is free from the restrictive assumption of long wavelengths of perturbations and can be easily generalized to the cases of $(2+1)$-dimensional cnoidal waves, multicomponent waves, and cnoidal waves in saturable optical media.

II. THEORETICAL MODEL

The propagation of optical pulses in the direction of longitudinal z axis in optical fibers is described by the dimensionless nonlinear Schrödinger equation for the complex field amplitude $q(\eta,\xi)$,

$$i\frac{\partial q}{\partial \xi}=\frac{d}{2}\frac{\partial^2 q}{\partial \eta^2}-|q|^2 q. \tag{1}$$

Here amplitude $q(\eta,\xi)=(L_{\mathrm{dis}}/L_{\mathrm{spm}})^{1/2}A(\eta,\xi)I_0^{-1/2}$; $A(\eta,\xi)$ is the slowly varying envelope of light field; I_0 is the input intensity; $\eta=(t-z/v_{\mathrm{gr}})/\tau_0$ is the normalized running time; τ_0 is the characteristic pulse duration; $v_{\mathrm{gr}}=(\partial k/\partial\omega)^{-1}_{\omega=\omega_0}$ is the group velocity; $\xi=z/L_{\mathrm{dis}}$ is the normalized propagation distance; $L_{\mathrm{dis}}=\tau_0^2/|\beta_2|$ is the dispersion length, corresponding to the chosen pulse duration τ_0; $\beta_2=(\partial^2 k/\partial\omega^2)_{\omega=\omega_0}$; $k_0=k(\omega_0)$ is the wave number; ω_0 is the carrying frequency; $L_{\mathrm{spm}}=2c/(\omega_0 n_2 I_0)$ is the self-phase modulation length; and $n_2=3\pi\omega_0\chi^{(3)}(\omega_0)/[k(\omega_0)c]$ is the nonlinear coefficient that is proportional to the Fourier transform $\chi^{(3)}(\omega_0)$ of the corresponding element of nonlinear susceptibility tensor. The first term in Eq. (1) describes the dispersion spreading and the second one accounts for self-focusing of optical pulse in the fiber. Parameter $d=-1$ corresponds to the anomalous dispersion regime, whereas $d=1$ corresponds to the normal dispersion regime.

Note that the distribution of the wave field on transverse coordinates in optical fibers is defined by the profiles of the guided modes. Hence the problem of stability of the cnoidal waves in optical fibers can be treated in $(1+1)$ dimensions. In the spatial case, Eq. (1) should be modified to include the derivatives with respect to two transverse coordinates. In this case a number of new effects come into play. Among these effects are transverse necklike and snakelike instabilities [46] that can develop along one of transverse axes even if the wave is stable in the frames of $(1+1)$-dimensional model described by Eq. (1) (which is valid also for slit laser beams). The analysis of stability for $(2+1)$-dimensional cnoidal waves (which are uniform, say, along the y axis and periodic along the x axis) is much more complicated than that for $(1+1)$-dimensional waves. We leave this problem for future consideration. Note that the method presented here can be easily modified in the case of $(2+1)$-dimensional cnoidal waves.

Equation (1) has two stationary periodic wave solutions in the anomalous dispersion regime $(d=-1)$ [24,25] (here we consider only fundamental periodic solutions of nonlinear Schrödinger equation):

$$\begin{aligned} q_{\mathrm{dn}}(\eta,\xi)&=\chi\,\mathrm{dn}[\chi(\eta-\eta_0-\alpha\xi),m]\\ &\quad\times\exp[i\alpha\eta+i\xi\chi^2(1-m^2/2)-(i/2)\alpha^2\xi+i\psi_0],\\ q_{\mathrm{cn}}(\eta,\xi)&=m\chi\,\mathrm{cn}[\chi(\eta-\eta_0-\alpha\xi),m]\\ &\quad\times\exp[i\alpha\eta+i\xi\chi^2(m^2-1/2)-(i/2)\alpha^2\xi+i\psi_0], \end{aligned} \tag{2}$$

and one stationary periodic wave solution in the normal dispersion regime $(d=1)$:

$$\begin{aligned} q_{\mathrm{sn}}(\eta,\xi)&=m\chi\,\mathrm{sn}[\chi(\eta-\eta_0-\alpha\xi),m]\\ &\quad\times\exp[-i\alpha\eta+i\xi\chi^2(1+m^2)/2+(i/2)\alpha^2\xi\\ &\quad+i\psi_0]. \end{aligned} \tag{3}$$

In expressions (2), (3) $\mathrm{cn}(\eta,m)$, $\mathrm{dn}(\eta,m)$, and $\mathrm{sn}(\eta,m)$ are elliptic functions; $0\leqslant m\leqslant 1$ is the modulus of the elliptic function that can be treated as a parameter describing the degree of localization of the wave field energy; χ is the arbitrary form factor; η_0 is the initial coordinate shift; α is the angle between the propagation direction and the longitudinal ξ axis (initial frequency shift); ψ_0 is the initial phase. Note that for the case of α, η_0, $\psi_0=0$ cnoidal waves (2) and (3) can be written in the general form $q(\eta,\xi)=w(\eta)\exp(ib\xi)$, with $w(\eta)$ being the real function that describes the wave profile, and b being the real propagation constant. We will use the general expression $q(\eta,\xi)=w(\eta)\exp(ib\xi)$ (with α, η_0, $\psi_0=0$) for cnoidal wave fields in the following section that is devoted to stability analysis. Besides the latter solution, Eq. (1) has a solution in the form of intrinsically complex or "chirped" cnoidal waves $q(\eta,\xi)=w(\eta)\exp[i\phi(\eta)\xi]$, where $\phi(\eta)$ is the real function of transverse coordinate η. Such waves are not considered in the present paper.

Functions $\mathrm{cn}(\eta,m)$ and $\mathrm{sn}(\eta,m)$ in expressions (2) and (3) have a sign-alternating oscillating character; function $\mathrm{dn}(\eta,m)$ is always positive and has the form of oscillations superimposed on the constant background. Period of cn and sn-waves equals to $4K(m)/\chi$, where $K(m)$ is the elliptical integral of the first kind, whereas period of dn-wave equals to $2K(m)/\chi$. The role of parameter m (in the following we will call it the localization parameter) can be easily interpreted for cn- and sn-waves. When $m\to 0$ wave amplitudes go to zero, provided that the nonlinear terms in Schrödinger equation (1) can be neglected. In this linear limiting case function $\mathrm{cn}(\eta,m)$ is well approximated by $\cos\eta$, and function $\mathrm{sn}(\eta,m)$ by $\sin\eta$ with periods equal to 2π. This is the case of a weak localization. With increase of m up to 1 the contribution of nonlinear terms in Eq. (1) increases, wave

periods go to infinity, and waves are transformed into a set of hyperbolic secant type solitons for cn-wave and hyperbolic tangent type solitons for sn-wave. This is the case of strong localization. dn-wave for $m \to 0$ transforms into a wave of constant amplitude and for $m \to 1$ into a set of hyperbolic secant type solitons, similarly to the case of cn-wave. Thus at α, η_0, $\psi_0 = 0$, one can write the following asymptotic expansions for functions in expressions (2) and (3):

$$q_{\mathrm{dn}}(\eta,\xi)|_{m\to 0} = \chi \exp(i\chi^2\xi),$$

$$q_{\mathrm{dn}}(\eta,\xi)|_{m\to 1} = \chi\, \mathrm{sech}(\chi\eta)\exp(i\chi^2\xi/2),$$

$$q_{\mathrm{cn}}(\eta,\xi)|_{m\to 0} = m\chi \cos(\chi\eta)\exp(-i\chi^2\xi/2),$$

$$q_{\mathrm{cn}}(\eta,\xi)|_{m\to 1} = \chi\, \mathrm{sech}(\chi\eta)\exp(i\chi^2\xi/2),$$

$$q_{\mathrm{sn}}(\eta,\xi)|_{m\to 0} = m\chi \sin(\chi\eta)\exp(i\chi^2\xi/2),$$

$$q_{\mathrm{sn}}(\eta,\xi)|_{m\to 1} = \chi \tanh(\chi\eta)\exp(i\chi^2\xi). \qquad (4)$$

Such properties of the cnoidal waves of cn-, sn-, and dn-types give one several intuitive hints about their stability. For example, one can suspect the instability of dn-wave, since it contains constant background that is modulationally unstable in the anomalous dispersion regime. Moreover, since in the limit of strong localization cnoidal waves are transformed into bright and dark solitons, instability (if it presents) should be suppressed for all types of cnoidal waves. Further throughout this paper we consider the case $\chi = 1$, since it is known that the solutions of Eq. (1) can be rescaled to any positive value of χ.

III. METHOD OF STABILITY ANALYSIS

To investigate the stability of periodic cnoidal waves we employ the well-known linear stability analysis that is valid (at least for exponentially growing perturbations) only at the initial stage of perturbation development. Note that earlier linear stability analysis was used mostly for fundamental soliton states [1–23], since there exists a common belief that for higher-order soliton states (having one or more nodes) the linear stability analysis enables to treat only very narrow class of perturbations that should go to zero in the nodes (zeros) of the higher-order solitons state. Upon consideration of the stability of periodical cnoidal waves one meets this difficulty from the very beginning, since waves of cn- and sn-types periodically change their signs and have unlimited number of nodes. We show that our analysis enables to find simultaneously perturbations that conform to the requirement of common zeros with corresponding cnoidal wave and perturbations that are nonzero in the wave nodes. Note also that the usual procedure of derivation of the VK stability criterion is inapplicable for the periodic cnoidal waves due to nonzero asymptotics of the wave field at infinity [2]. We will search for solutions of Eq. (1) that describe the propagation of the cnoidal wave with perturbed input profile in the following form:

$$q(\eta,\xi) = [w(\eta) + U(\eta,\xi) + iV(\eta,\xi)]\exp(ib\xi), \qquad (5)$$

where function $w(\eta)\exp(ib\xi)$ describes the evolution of the corresponding unperturbed wave as it was stated in the preceding section, functions $U(\eta,\xi)$ and $V(\eta,\xi)$ are, respectively, the real and imaginary parts of the small $(U,V \ll w)$ perturbation. For example, in the case of sn-wave (3) with α, η_0, $\psi_0 = 0$ and $\chi = 1$ (these parameter values will be used further in the paper) one has $w(\eta) = m\,\mathrm{sn}(\eta,m)$ and $b = (1 + m^2)/2$. For perturbations that are nonzero in the cnoidal wave nodes (for cn- and sn-waves), inequality $U, V \ll w$ breaks down only in the small areas around zeros of the cnoidal waves. For the wave of dn-type such difficulty does not arise because dn-wave is not equal to zero. Substitution of expression (5) into Schrödinger equation (1), subsequent linearization, and the derivation of the real and imaginary parts yields the following system of linear equations:

$$\frac{\partial U}{\partial \xi} = -\mathcal{L}V,$$

$$\frac{\partial V}{\partial \xi} = \mathcal{R}U. \qquad (6)$$

Here the linear operators $\mathcal{L} = -(d/2)(\partial^2/\partial\eta^2) + w^2(\eta) - b$ and $\mathcal{R} = \mathcal{L} + 2w^2(\eta)$ are both self-adjoint and depend on the transverse coordinate η, parameter d, and localization parameter m. The following properties $\mathcal{L}w = 0$, $\mathcal{R}(dw/d\eta) = 0$, and $\mathcal{R}(dw/db) = w$ can be easily verified by the direct substitution of functions w, $dw/d\eta$, and dw/db into the expressions for operators $\mathcal{L}$ and $\mathcal{R}$.

We will search for solutions of system (6) in the following form:

$$U(\eta,\xi) = \mathrm{Re}\left[\int C(\delta)u(\eta,\delta)\exp(\delta\xi)d\delta\right],$$

$$V(\eta,\xi) = \mathrm{Re}\left[\int C(\delta)v(\eta,\delta)\exp(\delta\xi)d\delta\right], \qquad (7)$$

where δ is the complex increment (growth rate) of perturbation; $C(\delta)$ are arbitrary complex constants; $u(\eta,\delta)$ and $v(\eta,\delta)$ are complex functions that describe the input profile of the perturbation and depend also on the increment value. Integration goes over all possible increment values. Under the substitution of expressions (7) into linear system (6) and the equation of underintegral terms with the same exponential coefficients $\exp(\delta\xi)$, one can get the following final system of linear equations with real linear operators $\mathcal{L}$ and $\mathcal{R}$:

$$\delta u = -\mathcal{L}v,$$

$$\delta v = \mathcal{R}u. \qquad (8)$$

Taking into account expressions for operators $\mathcal{L}$ and $\mathcal{R}$, one can rewrite the system of equations (8) in matrix form that is more convenient for subsequent analysis:

$$\frac{d\Phi}{d\eta} = \mathcal{B}\Phi, \quad \mathcal{B} = \begin{pmatrix} \mathcal{O} & \mathcal{E} \\ \mathcal{N} & \mathcal{O} \end{pmatrix},$$

$$\mathcal{N}=\begin{pmatrix} (6w^2-2b)/d & -2\delta/d \\ 2\delta/d & (2w^2-2b)/d \end{pmatrix}, \tag{9}$$

where $\Phi=\{u,v,du/d\eta,dv/d\eta\}^T$ is the solution vector; $\mathcal{O}$ is the 2×2 zero matrix; $\mathcal{E}$ is the 2×2 unity matrix; and only matrix $\mathcal{N}$ depends on the transverse coordinate η, increment δ, and parameters d and m. As one can see from Eq. (9), matrix $\mathcal{B}(\eta)$ can be presented in the form of Jordan's blocks. One of the most important properties of the matrix $\mathcal{B}$ is that $\mathrm{Tr}(\mathcal{B})=0$. The general solution of Eq. (9) can be written in the form

$$\Phi(\eta)=\mathcal{J}(\eta,\eta')\Phi(\eta'), \tag{10}$$

where $\mathcal{J}(\eta,\eta')$ is the 4×4 Cauchy matrix that can be found as a solution of the initial value problem $\partial\mathcal{J}(\eta,\eta')/\partial\eta=\mathcal{B}(\eta)\mathcal{J}(\eta,\eta')$, $\mathcal{J}(\eta',\eta')=\mathcal{E}$, where coordinate η' serves as a parameter. It is known that $\mathcal{J}(\eta,\eta')\mathcal{J}(\eta',\eta'')=\mathcal{J}(\eta,\eta'')$ and $\mathcal{J}(\eta',\eta)=\mathcal{J}^{-1}(\eta,\eta')$. Direct substitution shows that two matrices $\mathcal{B}(\eta)$ and $\mathcal{B}(\eta')$ are not commutative, and, hence, the general expression for Cauchy matrix can only be written in the form of "matrizant,"

$$\mathcal{J}(\eta,\eta')=\mathcal{E}+\sum_{k=1}^{\infty}\int_{\eta'}^{\eta}d\eta_1\int_{\eta'}^{\eta_1}d\eta_2\cdots\int_{\eta'}^{\eta_{k-1}}d\eta_k\mathcal{B}(\eta_1)\times\mathcal{B}(\eta_2)\cdots\mathcal{B}(\eta_k). \tag{11}$$

From expression $\mathrm{Tr}(\mathcal{B})=0$ it follows that the determinant of the matrix $\mathcal{J}(\eta,\eta')$ [which is the solution of the equation $\partial\mathcal{J}(\eta,\eta')/\partial\eta=\mathcal{B}(\eta)\mathcal{J}(\eta,\eta')$] is equal to unity for arbitrary values of coordinates η and η'. This important property will be used upon the analysis of Eq. (9). Further, one can take into account that $w(\eta)$ describing the cnoidal wave profile is the periodic function of coordinate η, i.e., $w(\eta+T)=w(\eta)$, where T is the wave period. This means that matrices $\mathcal{B}(\eta+T)=\mathcal{B}(\eta)$ and $\mathcal{J}(\eta+T,\eta'+T)=\mathcal{J}(\eta,\eta')$.

Let us define the matrix of "translation" of perturbation vector Φ on one period T,

$$\mathcal{P}(\eta)=\mathcal{J}(\eta+T,\eta), \tag{12}$$

and consider its properties. It follows from the definition of the matrix of translation that $\det[\mathcal{P}(\eta)]=1$ and $\mathcal{J}(\eta+kT,\eta)=\mathcal{P}^k(\eta)$, where k is an integer. Using the properties of the matrix $\mathcal{J}(\eta,\eta')$, one can show that

$$\mathcal{P}^k(\eta+\eta_0)=\mathcal{J}(\eta+\eta_0,\eta)\mathcal{P}^k(\eta)\mathcal{J}^{-1}(\eta+\eta_0,\eta) \tag{13}$$

for arbitrary values of η_0 and k. Characteristic polynom of translation matrix $D(\lambda)=\det[\mathcal{P}(\eta)-\lambda\mathcal{E}]$ and trace $\mathrm{Tr}[\mathcal{P}^k(\eta)]$ do not depend on coordinate η. Note that if λ_n $(n=1,...,4)$ are roots of the characteristic polynom, then $\det[\mathcal{P}(\eta)]=\lambda_1\lambda_2\lambda_3\lambda_4$ and $\mathrm{Tr}[\mathcal{P}(\eta)]=\lambda_1+\lambda_2+\lambda_3+\lambda_4$. Since $\det[\mathcal{P}(\eta)]=1$, all roots $\lambda_n\neq0$. Characteristic polynom of the matrix of translation can be written in the following general form:

$$D(\lambda)=\lambda^4+p_1\lambda^3+p_2\lambda^2+p_3\lambda+p_4. \tag{14}$$

Matrix $\mathcal{P}(\eta)$ satisfies its own characteristic equation $D(\mathcal{P})=\mathcal{P}^4+p_1\mathcal{P}^3+p_2\mathcal{P}^2+p_3\mathcal{P}+p_4\mathcal{E}=\mathcal{O}$. It also follows from equality $\det[\mathcal{P}(\eta)]=1$ that coefficient $p_4=1$. It is well known that coefficients p_k in expression (14) are connected with traces $T_k=\mathrm{Tr}[\mathcal{P}^k(\eta)]$ by the following relations (Newton's formulas):

$$T_k+p_1T_{k-1}+\cdots+p_{k-1}T_1=-kp_k \quad (k=1,...,4), \tag{15}$$

where T_k and p_k are independent of the transverse coordinate η, as it was shown above.

Using expression (11) for Cauchy matrix $\mathcal{J}(\eta,\eta')$, one can easily show that $\mathrm{Tr}[\mathcal{J}(\eta,\eta')]=\mathrm{Tr}[\mathcal{J}^{-1}(\eta,\eta')]$ for arbitrary values of η and η' (see Appendix A for details). Since $\mathcal{J}(\eta,\eta')=\mathcal{J}^{-1}(\eta',\eta)$, it follows from the previous expression that equality $\mathrm{Tr}[\mathcal{P}^k(\eta)]=\mathrm{Tr}[\mathcal{P}^{-k}(\eta)]$ and, hence, equality $T_k=T_{-k}$ hold for all values of k, where k is an integer. Multiplying equation $D(\mathcal{P})=\mathcal{O}$ with $\mathcal{P}^{-k}$, where $k=1,...,4$, and calculating traces of the left and right parts of resulting equations, we get four expressions [additionally to expressions (15)] connecting parameters p_k and T_k. Resulting system of eight equations (see Appendix B) for p_k and T_k, together with $p_4=1$, is consistent only when

$$p_1=-T_1,\qquad p_2=-\tfrac{1}{2}(T_2-T_1^2),\qquad p_3=-T_1,\qquad p_4=1. \tag{16}$$

Traces $T_3=T_1(3+3T_2/2-T_1^2/2)$ and $T_4=4(T_1^2-1)+T_2^2/2+T_1^2T_2-T_1^4/2$ are also expressible through lowest-order traces T_1 and T_2. Characteristic polynom of the translation matrix (14) and its roots take finally very simple form:

$$D(\lambda)=\lambda^4-T_1\lambda^3-\tfrac{1}{2}(T_2-T_1^2)\lambda^2-T_1\lambda+1,$$

$$\lambda_1=\tfrac{1}{4}[T_1+(2T_2-T_1^2+8)^{1/2}]+\{\tfrac{1}{16}[T_1+(2T_2-T_1^2+8)^{1/2}]^2-1\}^{1/2},$$

$$\lambda_2=\tfrac{1}{4}[T_1-(2T_2-T_1^2+8)^{1/2}]+\{\tfrac{1}{16}[T_1-(2T_2-T_1^2+8)^{1/2}]^2-1\}^{1/2},$$

$$\lambda_3=1/\lambda_1,\qquad \lambda_4=1/\lambda_2. \tag{17}$$

Expressions (17) give us nonzero eigenvalues λ_n $(n=1,...,4)$ of the matrix of translation $\mathcal{P}(\eta)$. Eigenvectors $\Phi_n(\eta)$ corresponding to the eigenvalues λ_n can be found as solutions of the linear problems $\mathcal{P}(\eta)\Phi_n(\eta)=\lambda_n\Phi_n(\eta)$. Note that eigenvectors of the matrix $\mathcal{J}(\eta+kT,\eta)=\mathcal{P}^k(\eta)$ of translation on k periods coincide with eigenvectors $\Phi_n(\eta)$ of the matrix $\mathcal{P}(\eta)$, whereas its eigenvalues are given by λ_1^k, λ_2^k, λ_3^k, λ_4^k.

Let us consider two distinct situations when all eigenvalues λ_n of the matrix $\mathcal{P}(\eta)$ of translation on one period are different and when repeated eigenvalues are possible. Since eigenvectors of the matrix $\mathcal{J}(\eta+kT,\eta)$ coincide with eigenvectors $\Phi_n(\eta)$ of matrix $\mathcal{P}(\eta)$, vector $\Phi(\eta)$ that is the solution of Eq. (9) and that satisfies expression (10) can be uniquely expressed through the eigenvectors of matrix $\mathcal{P}(\eta)$:

$$\Phi(\eta)=\sum_{n=1}^{4} C_n\Phi_n(\eta), \tag{18}$$

because in the case of distinct eigenvalues λ_n eigenvectors $\Phi_n(\eta)$ form basis in the vector space where Cauchy matrix $\mathcal{J}(\eta,\eta')$ acts. In expression (18) C_n are the arbitrary complex coefficients. Applying the matrix of translation on k periods to the vector (18), one obtains

$$\Phi(\eta+kT)=\mathcal{J}(\eta+kT,\eta)\Phi(\eta)=\sum_{n=1}^{4} C_n\lambda_n^k\Phi_n(\eta). \tag{19}$$

Expression (19) gives one an obvious criterion of searching of perturbation vectors $\Phi(\eta)$ that remain limited for arbitrary value of transverse coordinate η. According to this criterion, upon construction of arbitrary perturbation vectors one should choose in expansion (18) only eigenvectors $\Phi_n(\eta)$ that correspond to $|\lambda_n|=1$. Inclusion into expression (18) eigenvectors $\Phi_n(\eta)$ with $|\lambda_n|\neq 1$ leads in accordance with Eq. (19) to unlimited increase of the perturbation amplitude at $\eta\rightarrow\pm\infty$.

The situation is more complicated in the case of repeated eigenvalues of matrix $\mathcal{P}(\eta)$, because eigenvectors $\Phi_n(\eta)$ in general case cannot serve as a basis in vector space where matrix $\mathcal{J}(\eta,\eta')$ acts. In the case of repeated eigenvalues characteristic polynom (14) takes the following form:

$$D(\lambda)=\prod_{n=1}^{r}(\lambda-\lambda_n)^{m_n},\quad \sum_{n=1}^{r} m_n=4, \tag{20}$$

where $1\leqslant r\leqslant 4$ is the number of distinct eigenvalues, m_n is the multiplicity of eigenvalue λ_n. Using expression (20) and substituting in polynom $D(\lambda)$ the matrix of translation $\mathcal{P}(\eta)$ instead of λ, one can show that the vector space $\mathcal{S}$ where matrix $\mathcal{J}(\eta,\eta')$ acts can be decomposed into a direct sum of subspaces $\mathcal{S}_1,\ldots,\mathcal{S}_r$, where subspace $\mathcal{S}_n$ consists of vectors satisfying the condition

$$[\mathcal{P}(\eta)-\lambda_n\mathcal{E}]^{m_n}\Phi_n(\eta)=\mathcal{O}. \tag{21}$$

Here $\mathcal{E}$ is the 4×4 unity matrix and $\mathcal{O}$ is a 4×1 zero vector. Arbitrary perturbation vector $\Phi(\eta)$ that belongs to vector space $\mathcal{S}$ can, therefore, be expressed as a sum of vectors $\Phi_n(\eta)$ belonging to subspaces $\mathcal{S}_n$,

$$\Phi(\eta)=\sum_{n=1}^{r}\Phi_n(\eta), \tag{22}$$

where all $\Phi_n(\eta)$ satisfy conditions (21). Note that in the right part of expansion (22) one can use vectors $C_n\Phi_n(\eta)$ with arbitrary complex coefficients C_n instead of $\Phi_n(\eta)$. Applying to vector (22) the matrix of translation on k periods $\mathcal{J}(\eta+kT,\eta)$, after some simple algebra we arrive at a formula

$$\Phi(\eta+kT)=\mathcal{J}(\eta+kT,\eta)\Phi(\eta)=\sum_{n=1}^{r}\lambda_n^k\sum_{m=0}^{k}C_k^m\lambda_n^{-m}[\mathcal{P}(\eta)-\lambda_n\mathcal{E}]^m\Phi_n(\eta). \tag{23}$$

Here $C_k^m=k!/m!(k-m)!$ are the binomial coefficients and we suppose that $k>0$. Note that for $k\geqslant 4$ summation on m in Eq. (23) can be carried out from 0 up to m_n since $[\mathcal{P}(\eta)-\lambda_n\mathcal{E}]^m\Phi_n(\eta)=\mathcal{O}$ for $m>m_n$ in accordance with expression (21). An analogous expression can be easily obtained for $k<0$. It follows from Eq. (23) that similarly to the case of distinct eigenvalues λ_n of matrix $\mathcal{P}(\eta)$ in the case of repeated eigenvalues perturbation vector $\Phi(\eta)$ remains limited when one uses in formula (22) only such vectors $\Phi_n(\eta)$ that correspond to $|\lambda_n|=1$ and satisfy conditions (21). Note also that binomial coefficient C_k^m in Eq. (23) remains limited with increase of k only for $m=0$ and $m=k$. This fact put the additional (except requirement $|\lambda_n|=1$) condition

$$\mathcal{P}(\eta)\Phi_n(\eta)=\lambda_n\Phi_n(\eta) \tag{24}$$

on the vectors $\Phi_n(\eta)$ in Eq. (23) that is more general than Eq. (21) and coincides with condition defining eigenvectors and eigenvalues of the matrix of translation $\mathcal{P}(\eta)$.

Thus for both cases of distinct and repeated eigenvalues of translation matrix, perturbation vector can be obtained as an expansion on the eigenvectors of translation matrix

$$\Phi(\eta)=\sum_{\substack{n=1,\\ |\lambda_n|=1}}^{r} C_n\Phi_n(\eta), \tag{25}$$

where $1\leqslant r\leqslant 4$ is the number of distinct eigenvalues and summation goes over eigenvalues with $|\lambda_n|=1$.

Searching for the profiles of perturbation vectors corresponding to the various cnoidal waves, localization parameters m and increments δ, we first constructed matrix $\mathcal{B}$, and then calculated matrices $\mathcal{J}(\eta,\eta')$ and $\mathcal{P}(\eta)$ numerically. After that eigenvalues of the matrix $\mathcal{P}(\eta)$ conforming to the condition $|\lambda_n|=1$ were found and eigenvectors $\Phi_n(\eta)$ were built.

To search the areas on the complex δ plane where one of the conditions $|\lambda_n|=1$ is satisfied, we fixed $|\delta|$ and scanned $\arg(\delta)$ with the fine step (typically $\sim 2\pi/1000$). Then scanning procedure was repeated for a slightly increased value of $|\delta|$ (step ~ 0.001); the segment of $|\delta|$ scanning was [0,100]. For purely real or imaginary increments $|\lambda_n(\delta)|$ may be equal to unity in the points where $\arg(\delta)=0$ or $\arg(\delta)=\pi/2$, correspondingly. To find the point in which $|\lambda_n(\delta)|$ goes to unity in the case of complex increments δ we arranged one-dimensional search along $\arg(\delta)$ axis. In all practical cases dependence $|\lambda_n(\delta)|$ on $\arg(\delta)$ has a single well-defined maximum, corresponding to condition $|\lambda_n|=1$.

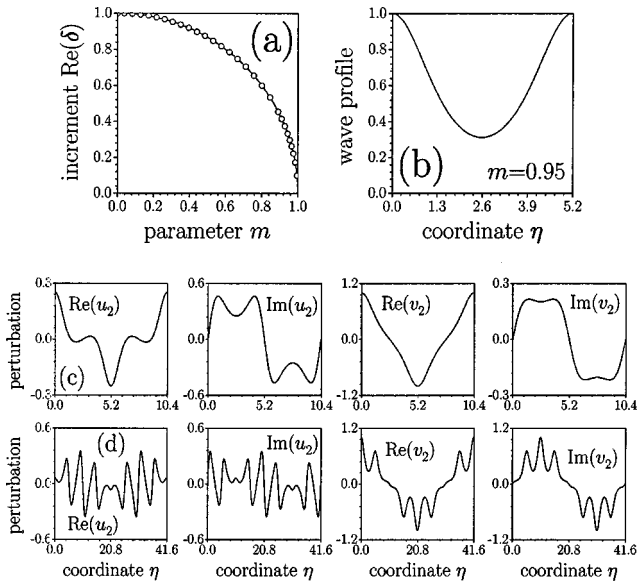

FIG. 1. (a) Areas of existence of limited perturbations for dn-wave in the case of purely real increment δ. In the area below the line with circles both $|\lambda_1|=1$ and $|\lambda_2|=1$. In the area above the line with circles both $|\lambda_1|\neq 1$ and $|\lambda_2|\neq 1$. (b) shows the profile of dn-wave for $m=0.95$. Row (c) shows the profile of perturbation corresponding to increment $\mathrm{Re}(\delta)=0.283\,22$ and localization parameter $m=0.95$. Row (d) shows the profile of perturbation corresponding to $\mathrm{Re}(\delta)=0.083\,41$ and $m=0.95$.

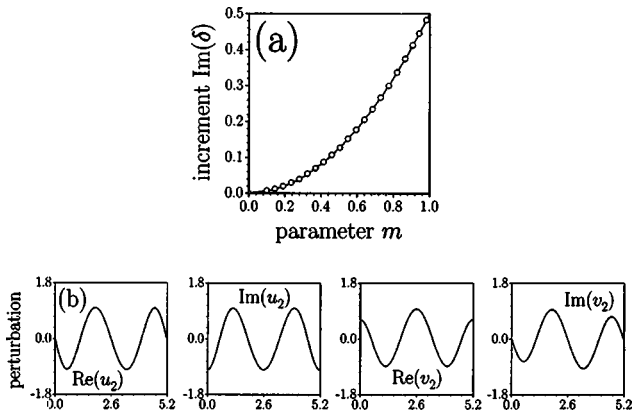

FIG. 2. (a) Areas of existence of limited perturbations for dn-wave in the case of purely imaginary increment δ. In (a) $|\lambda_1|\neq 1$ everywhere, whereas $|\lambda_2|=1$ in the area above the line with circles. Row (b) shows the profile of perturbation corresponding to increment $\mathrm{Im}(\delta)=2.6244$ and localization parameter $m=0.95$.

Careful numerical analysis shows that for mixed increments δ with $\mathrm{Re}(\delta)\mathrm{Im}(\delta)\neq 0$ conditions $|\lambda_n|=1$ are satisfied only in the case of cn-wave for small values of $|\delta|$. For the waves of sn and dn-types conditions $|\lambda_n|=1$ are satisfied only for purely real or purely imaginary increments. Moreover, in contradiction with the case of localized fundamental soliton pulses in the case of periodic cnoidal waves, the spectrum of possible increment values is continuous, i.e., for fixed localization parameter *m* there exists unlimited number of perturbations corresponding to different increments. Further throughout this paper we consider perturbations corresponding to eigenvalues λ_1 and λ_2 from formula (17) since from $|\lambda_1|=1$ it follows that $|\lambda_3|=1$ and from $|\lambda_2|=1$ it follows that $|\lambda_4|=1$. Moreover, profiles of perturbations corresponding to eigenvalues $\lambda_{3,4}$ can be easily found from known profiles of perturbations for eigenvalues $\lambda_{1,2}$ if one take into account the following relations: $u_n(\eta)=u_{n+2}(-\eta)$ and $v_n(\eta)=v_{n+2}(-\eta)$, where $n=1,2$.

IV. RESULTS AND DISCUSSION

First we concentrate on the case of dn-wave described by the first of expressions (2). Figure 1(a) shows the areas of existence of limited perturbations [areas at the plane (m,δ) where at least one of eigenvalues conforms to the requirement $|\lambda_n|=1$] for dn-wave in the case of purely real increment δ. One can see from the figure that in the area below the line with circles [this line is very well described by the equation $\mathrm{Re}^2(\delta)+m^2=1$] both $|\lambda_{1,2}|=1$. This fact means that dn-wave is *unstable* in the whole range of its existence. Instability can be associated with the presence of the constant background in dn-wave that is modulationally unstable in the anomalous dispersion regime. However, with increase of the localization parameter *m* up to unity when dn-wave is transformed into the set of well-separated bright solitons and constant background vanishes, the width of instability area along δ axis decreases. For $m=1$ dn-wave becomes stable, which is in consistence with the well-known stability of isolated $(1+1)$-dimensional solitons in the cubic media. Figure 1(b) shows the typical profile of dn-wave, whereas Figs. 1(c) and 1(d) show profiles of perturbations corresponding to this wave, eigenvalue λ_2, and two different increment values. All perturbations are presented in a normalized form for convenience. Since the spectrum of possible increment values is continuous, it is possible to find perturbations with various periods. The most interesting are the perturbations with periods that are divisible by period of the cnoidal wave. Perturbation with period that is two times bigger then the period of dn-wave is shown in Fig. 1(c) and it has the minimal possible period. Period of perturbation from Fig. 1(d) is eight times higher than the wave period. Two characteristic scales are clearly seen from this figure: one is equal to the perturbation period, whereas second equals the period of dn-wave.

Figure 2(a) shows the areas of existence of limited perturbations for dn-wave in the case of purely imaginary increment δ. In this figure $|\lambda_1|\neq 1$ everywhere, whereas $|\lambda_2|=1$ in the area above the line with circles [this line is very well described by the equation $\mathrm{Im}(\delta)=m^2/2$]. Perturbation shown in Fig. 2(b) has the same period as the dn-wave. Once again, two characteristic scales are clearly visible; however, now period of dn-wave defines the highest of these two scales. Note that when $m\to 0$ the profiles of perturbation are very well described by harmonic functions.

Results obtained with the aid of linear stability analysis are confirmed by the results of direct numerical integration of Eq. (1) by split-step Fourier method. Initial conditions were set in the form (5) with $U(\eta,\xi=0)$ and $V(\eta,\xi=0)$ being the small perturbations of the input wave that are found from Eqs. (7)–(9). Figure 3(a) shows the evolution of the perturbation $|\delta q(\eta,\xi)|$ with propagation in the case of

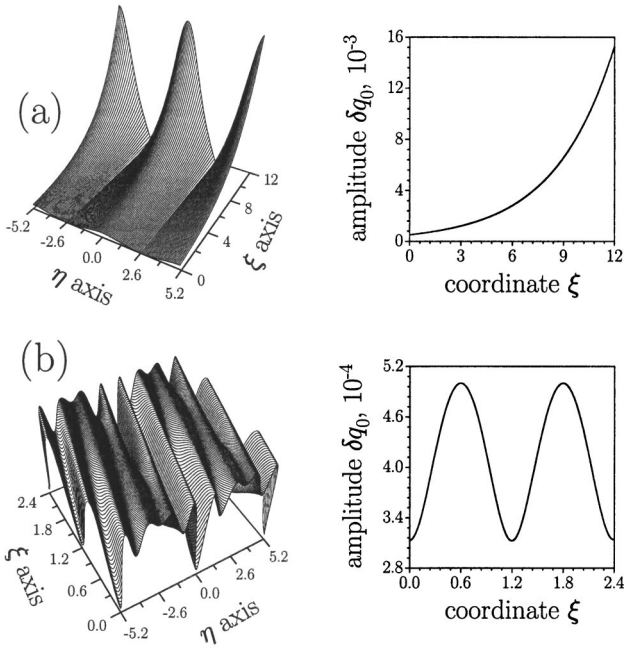

FIG. 3. Row (a) shows the initial stage of evolution of perturbation of dn-wave depicted in row (c) of Fig. 1 and corresponding to the real increment $\mathrm{Re}(\delta)=0.283\,22$. Row (b) shows the evolution of perturbation of dn-wave depicted in row (b) of Fig. 2 and corresponding to the imaginary increment $\mathrm{Im}(\delta)=2.6244$. Localization parameter $m=0.95$. Two-dimensional plots show the dependence of perturbation amplitude on the propagation distance.

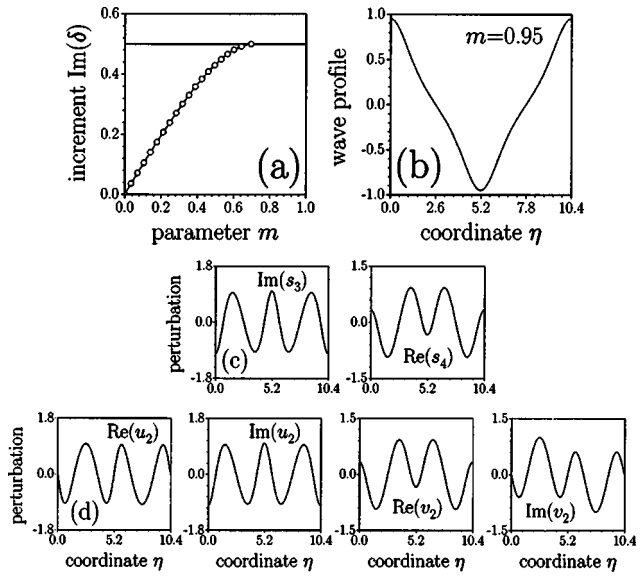

FIG. 4. (a) Areas of existence of limited perturbations for cn-wave in the case of purely imaginary increment δ. $|\lambda_1|=1$ in the area between the horizontal line and the line with circles. $|\lambda_2|=1$ in the area above the horizontal line and the line with circles. (b) shows the profile of cn-wave for $m=0.95$. Row (c) shows the profile of perturbation obtained from the linear combination for $\mathrm{Im}(\delta)=1.3967$. Row (d) shows the profile of perturbation that was used for the construction of perturbation depicted in row (c). Parameter $m=0.95$ for rows (c) and (d).

purely real increment δ. Perturbation $|\delta q(\eta,\xi)|$ grows exponentially upon propagation. Two-dimensional plots show the dependence of amplitude $\delta q_0=|\delta q(\eta=0,\xi)|$ of perturbation on the distance ξ. Figure 3(b) shows the evolution of perturbation corresponding to purely imaginary increment δ. Perturbation periodically restores its input profile and "drifts" along the dn-wave in the process of propagation. As one can see from the two-dimensional plot in row (b) frequency of oscillations of $\delta q_0(\xi)$ is exactly two times higher than the actual increment value δ. This discrepancy is connected with the procedure of modulus calculation for the complex field $\delta q(\eta,\xi)$.

Note that in the limiting case of $|\delta|\to 0$, when perturbation period greatly exceeds the period of corresponding dn-wave, our results are in excellent agreement with the results of papers [39,42] devoted to the analysis of stability of cnoidal waves in the approximation of long-wavelength perturbations.

Next we concentrate on the analysis of stability of cn-wave. In the case of cn-wave condition $|\lambda_n|=1$ is satisfied for purely imaginary increments and for complex increments with nonzero real and imaginary parts. Complex increments corresponding to $|\lambda_n|=1$ can be found for all values of localization parameter except the limiting case when $m=1$. Thus one can conclude that cn-wave is *unstable* in the whole domain of its existence.

Areas of existence of limited perturbations for cn-wave in the case of purely imaginary increments are shown in Fig. 4(a). Here $|\lambda_1|=1$ in the area between the horizontal line $\delta=1/2$ and the line with circles. The latter line ends at the point where $m=2^{-1/2}$. $|\lambda_2|=1$ everywhere in the area above the horizontal line $\delta=1/2$ and the line with circles. Figure 4(b) shows the typical profile of cn-wave. As it was mentioned above upon consideration of the stability of waves of cn- and sn-types, one faces the difficulty connected with the justification of the applicability of linearization procedure around the wave nodes. Analysis shows that perturbation components $u_n(\eta)$ and $v_n(\eta)$ calculated for cn-wave in accordance with the procedure described above are *always* nonzero in the wave nodes. However, it follows from expression (25) that linear combination of eigenvectors can also be treated as a perturbation instead of single eigenvector $\Phi_n(\eta)$ that was used in the case of dn-wave. Taking into account the symmetry properties $u_n(\eta)=u_{n+2}(-\eta)$ and $v_n(\eta)=v_{n+2}(-\eta)$, where $n=1,2$, we used for the further analysis vector combinations $\Sigma_1(\eta)=[\Phi_1(\eta)+\Phi_3(\eta)]/2$, $\Sigma_2(\eta)=[\Phi_2(\eta)+\Phi_4(\eta)]/2$, $A_1(\eta)=i[\Phi_1(\eta)-\Phi_3(\eta)]/2$, and $A_2(\eta)=i[\Phi_2(\eta)-\Phi_4(\eta)]/2$. These vector combinations have components:

$$\begin{aligned}
&\Sigma_1, \quad s_1=(u_1+u_3)/2, \quad s_2=(v_1+v_3)/2,\\
&\Sigma_2, \quad s_3=(u_2+u_4)/2, \quad s_4=(v_2+v_4)/2,\\
&A_1, \quad a_1=i(u_1-u_3)/2, \quad a_2=i(v_1-v_3)/2,\\
&A_2, \quad a_3=i(u_2-u_4)/2, \quad a_4=i(v_2-v_4)/2.
\end{aligned} \tag{26}$$

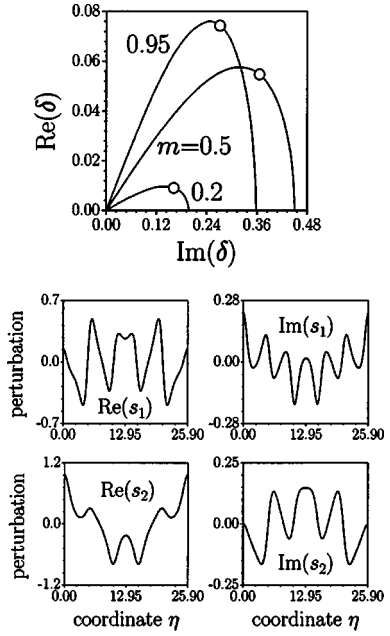

FIG. 5. Upper plot shows curves at the plane of complex increments where one of the conditions $|\lambda_{1,2}|=1$ is satisfied for cn-wave. For the left parts of these curves (before points marked by circles) $|\lambda_1|=1$, $|\lambda_2|\neq 1$, whereas right parts of these curves (after points marked by circles) correspond to $|\lambda_2|=1$, $|\lambda_1|\neq 1$. Four lower plots show the profile of perturbation corresponding to increment $\delta=0.075\,15+0.223\,58i$ and cn-wave with $m=0.95$.

One of the advantages of using such combinations is that usually one of the real or imaginary parts of functions $s_n(\eta)$, $a_n(\eta)$ goes to zero. Figure 4(c) shows the perturbation profile for vector combination $\Sigma_2(\eta)$ [with components $s_3(\eta)$ and $s_4(\eta)$], cn-wave depicted in Fig. 4(b), and eigenvalue $\lambda_2=-1$. Only nonzero perturbation components are presented. One can see from the figure that functions $s_{3,4}(\eta)$ are zero in the nodes of corresponding cn-wave. This is the method of construction of perturbations that formally satisfy linearization procedure in the case of cn- and sn-waves for arbitrary values of coordinate η. Finally, Fig. 4(d) shows the components $u_2(\eta)$, $v_2(\eta)$ of vector $\Phi_2(\eta)$ that were used for the construction of vector $\Sigma_2(\eta)$ having components depicted in Fig. 4(c).

The case of cn-wave is unique in the sense that only for such waves one can find perturbations corresponding to complex increments with $\mathrm{Re}(\delta)\mathrm{Im}(\delta)\neq 0$. Numerical analysis shows that at fixed localization parameter m, all possible increments lie on the certain curve at the $[\mathrm{Re}(\delta),\mathrm{Im}(\delta)]$ plane (see Fig. 5). Note that left parts of the curves in Fig. 5 (before points marked by circles) correspond to $|\lambda_1|=1$, $|\lambda_2|\neq 1$, whereas right parts correspond to $|\lambda_2|=1$, $|\lambda_1|\neq 1$. One can see that conditions $|\lambda_n|=1$ are satisfied only for relatively small $|\delta|$. Instability of cn-wave is suppressed in two limiting cases when $m\to 0$ and $m\to 1$. Typical profile of perturbation corresponding to mixed increment δ and vector combination $\Sigma_1(\eta)$ is also shown in Fig. 5.

Results of the numerical integration of Eq. (1) confirm the predictions of analytical approach. Figure 6(a) shows the evolution of perturbation $\Sigma_2(\eta)$ depicted in Fig. 4(c) upon

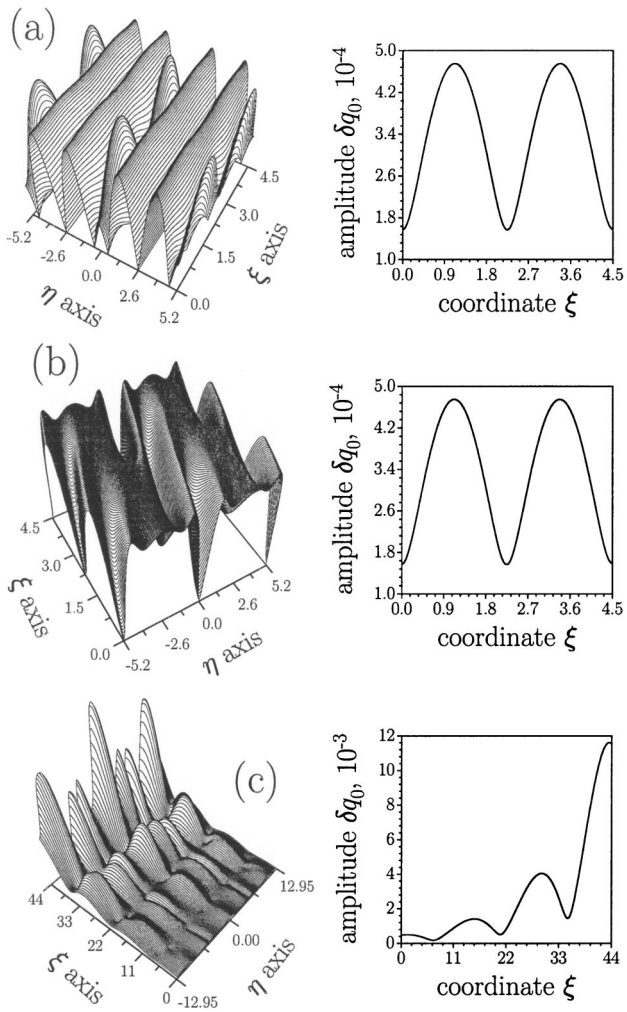

FIG. 6. Row (a) shows the evolution of perturbation of cn-wave depicted in row (c) of Fig. 4 and corresponding to the imaginary increment $\mathrm{Im}(\delta)=1.3967$. Row (b) shows the evolution of perturbation of cn-wave depicted in row (d) of Fig. 4 and corresponding to the same increment value. Evolution of perturbation that is plotted in Fig. 5 for $\delta=0.075\,15+0.223\,58i$ is presented in row (c). Localization parameter $m=0.95$. Two-dimensional plots show the dependence of perturbation amplitude on the propagation distance.

propagation. For comparison, in Fig. 6(b) we presented the evolution of perturbation $\Phi_2(\eta)$ with components $u_2(\eta)$, $v_2(\eta)$ that are nonzero in the wave nodes [see Fig. 4(d)] and that were used for the construction of $\Sigma_2(\eta)$. Note that perturbation $\Phi_2(\eta)$ ''drifts'' along the cn-wave, whereas $\Sigma_2(\eta)$ ''follows'' the cnoidal wave upon propagation. Moreover, despite the fact that formally linearization is inapplicable for $\Phi_2(\eta)$ in the wave nodes, numerical simulation gives absolutely identical results for $\Phi_2(\eta)$ and $\Sigma_2(\eta)$. This conclusion holds for all values of localization parameter m and increment δ. Therefore, one can make important conclusion that linearization technique *can be used* for waves and higher-order solitons with nodes. Figure 6(c) shows the evolution of perturbation $\Sigma_1(\eta)$ of cn-wave depicted in Fig. 5 and corresponding to complex increment δ. One can clearly

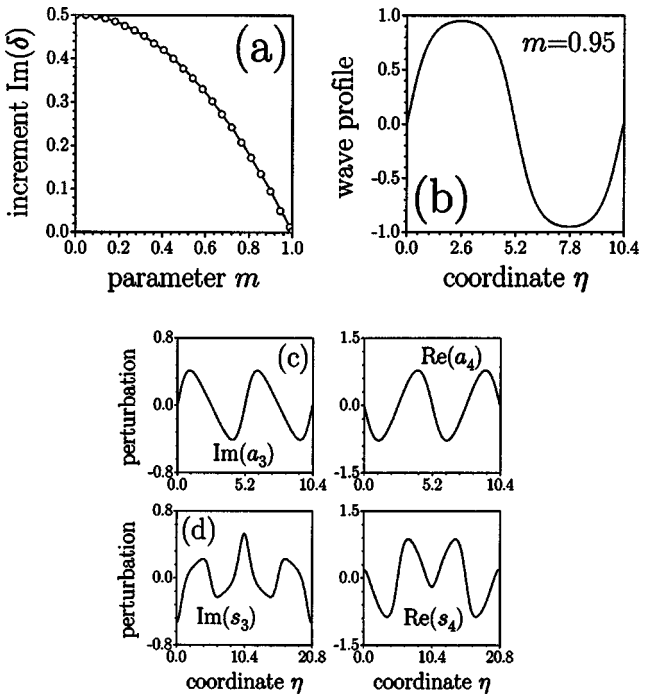

FIG. 7. (a) Areas of existence of limited perturbations for sn-wave in the case of purely imaginary increment δ. $|\lambda_1|=1$ in the area below line with circles, whereas $|\lambda_2|=1$ everywhere. (b) shows the profile of sn-wave for $m=0.95$. Rows (c) and (d) show the profiles of perturbations obtained from linear combinations for $\mathrm{Im}(\delta)=0.7808$ and $\mathrm{Im}(\delta)=0.374\,25$, respectively. For perturbations shown in rows (c) and (d), localization parameter $m=0.95$.

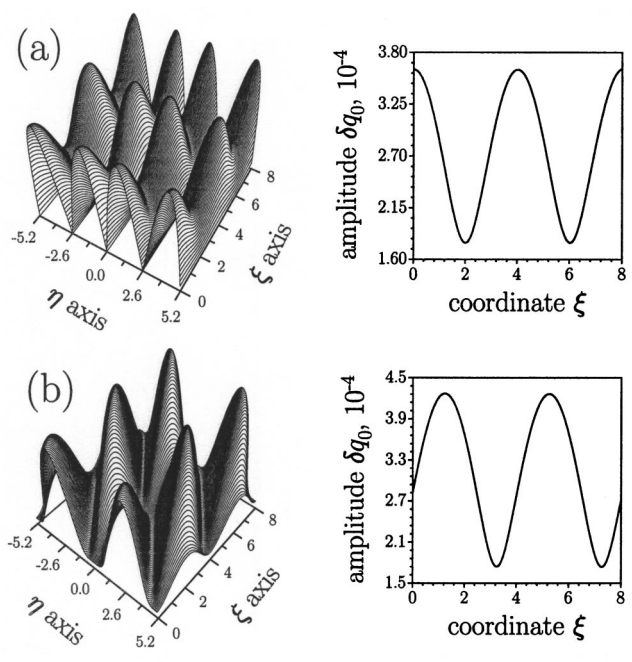

FIG. 8. Row (a) shows the evolution of perturbation of sn-wave depicted in row (c) of Fig. 7 and corresponding to the imaginary increment $\mathrm{Im}(\delta)=0.7808$. Row (b) shows the evolution of perturbation of sn-wave that was used for the construction of perturbation depicted in row (c) of Fig. 7. Localization parameter $m=0.95$. Two-dimensional plots show the dependence of perturbation amplitude on the propagation distance.

see the exponentially growing oscillations of perturbation amplitude.

Areas of existence of limited perturbations for the case of sn-wave are presented in Fig. 7(a). For real and mixed increments δ there are no eigenvalues conforming to the conditions $|\lambda_n|=1$. This means that sn-wave is *stable* in the whole domain of its existence. It is interesting that now $|\lambda_2|=1$ in the whole plane (m,δ), whereas $|\lambda_1|=1$ in the area lying below the line with circles [this line is well described by the equation $\mathrm{Im}(\delta)=(1-m^2)/2$]. Typical profile of sn-wave is shown in Fig. 7(b) whereas characteristic perturbation profiles are depicted in Fig. 7(c) [perturbation corresponding to vector combination $A_2(\eta)$] and Fig. 7(d). Evolution of perturbation presented in Fig. 7(c) is shown in Fig. 8(a), whereas Fig. 8(b) illustrates the evolution of perturbation $\Phi_2(\eta)$ that was used for the construction of $A_2(\eta)$. In the case of sn-wave we once again got the confirmation of the applicability of linearization technique for the analysis of stability of cnoidal waves with nodes since frequencies of oscillations of perturbation amplitude δq_0 coincide for perturbation $A_2(\eta)$ that is zero in the wave nodes and perturbation $\Phi_2(\eta)$ that is nonzero in the wave nodes.

V. CONCLUSION

We analyzed the stability of periodic cnoidal waves of cn-, dn-, and sn-types. It was shown that dn- and cn-waves are *unstable*, whereas sn-wave is *stable* with respect to the small perturbations of input profiles. The width of instability area for dn-wave decreases when $m\to 1$ and in the limit of strong localization when dn-wave transforms into the set of localized bright solitons, it becomes stable. Instability of cn-wave is suppressed for $m\to 0$ and $m\to 1$. We showed that the linearization technique is applicable for the analysis of stability of waves with nodes. The method of analysis of stability of periodic waves developed here is based on the construction of Cauchy matrix for perturbation vector and calculation of eigenvalues of this matrix. It enables one to formulate the criteria of existence of limited perturbations for a given increment value and hence to make a conclusion about stability or instability of the corresponding cnoidal waves. This method can be readily applied for the investigation of stability of multicomponent and multicolor $(1+1)$-dimensional cnoidal waves, as well as for $(2+1)$-dimensional waves.

ACKNOWLEDGMENTS

Yaroslav V. Kartashov acknowledges support from the Generalitat de Catalunya. Financial support from CONACYT under Grant No. 34684-E is gratefully acknowledged by Victor A. Vysloukh.

APPENDIX A

In this appendix we show that equality $\mathrm{Tr}[\mathcal{J}(\eta,\eta')]=\mathrm{Tr}[\mathcal{J}^{-1}(\eta,\eta')]$ holds for all values of coordinates η and

η'. It can be easily shown that inverse matrix $\mathcal{J}^{-1}(\eta,\eta')$ satisfies the equation $\partial\mathcal{J}^{-1}(\eta,\eta')/\partial\eta = -\mathcal{J}^{-1}(\eta,\eta')\mathcal{B}(\eta)$, since matrix $\mathcal{J}(\eta,\eta')$ satisfies the equation $\partial\mathcal{J}(\eta,\eta')/\partial\eta=\mathcal{B}(\eta)\mathcal{J}(\eta,\eta')$. Analogously to expression (11), a general expression for the inverse Cauchy matrix can be written in the form of "matrizant:"

$$\mathcal{J}^{-1}(\eta,\eta')=\mathcal{E}+\sum_{k=1}^{\infty}(-1)^k\int_{\eta'}^{\eta}d\eta_1\int_{\eta'}^{\eta_1}d\eta_2\cdots \times\int_{\eta'}^{\eta_{k-1}}d\eta_k\mathcal{B}(\eta_k)\mathcal{B}(\eta_{k-1})\cdots\mathcal{B}(\eta_1). \tag{A1}$$

Here $\mathcal{E}$ is a 4×4 unity matrix. Note the inverse order of arguments of matrices $\mathcal{B}(\eta_k)$ under the integral signs in expression (A1) in comparison with expression (11). Considering traces of matrices $\mathcal{J}(\eta,\eta')$ and $\mathcal{J}^{-1}(\eta,\eta')$, one gets

$$\begin{aligned}\mathrm{Tr}[\mathcal{J}(\eta,\eta')]&=4+\sum_{k=1}^{\infty}\int_{\eta'}^{\eta}d\eta_1\int_{\eta'}^{\eta_1}d\eta_2\cdots\int_{\eta'}^{\eta_{k-1}}d\eta_k \times\mathrm{Tr}[\mathcal{B}(\eta_1)\mathcal{B}(\eta_2)\cdots\mathcal{B}(\eta_k)],\\ \mathrm{Tr}[\mathcal{J}^{-1}(\eta,\eta')]&=4+\sum_{k=1}^{\infty}(-1)^k\int_{\eta'}^{\eta}d\eta_1\int_{\eta'}^{\eta_1}d\eta_2\cdots \times\int_{\eta'}^{\eta_{k-1}}d\eta_k\mathrm{Tr}[\mathcal{B}(\eta_k)\mathcal{B}(\eta_{k-1})\cdots\mathcal{B}(\eta_1)].\end{aligned} \tag{A2}$$

It is well known that $\mathrm{Tr}[\mathcal{B}(\eta_1)\mathcal{B}(\eta_2)\cdots\mathcal{B}(\eta_k)] = \mathrm{Tr}[\mathcal{B}^T(\eta_k)\mathcal{B}^T(\eta_{k-1})\cdots\mathcal{B}^T(\eta_1)]$. It can be checked by direct substitution that matrix $\mathcal{B}^T(\eta)=\mathcal{K}^{-1}\mathcal{B}(\eta)\mathcal{K}$, where matrix $\mathcal{K}$ is given by

$$\mathcal{K}=\begin{pmatrix}\mathcal{O}&\mathcal{I}\\ \mathcal{I}&\mathcal{O}\end{pmatrix},\quad \mathcal{I}=\begin{pmatrix}1&0\\0&-1\end{pmatrix}. \tag{A3}$$

This fact enables us to conclude that

$$\mathrm{Tr}[\mathcal{B}(\eta_1)\mathcal{B}(\eta_2)\cdots\mathcal{B}(\eta_k)]=\mathrm{Tr}[\mathcal{B}(\eta_k)\mathcal{B}(\eta_{k-1})\cdots\mathcal{B}(\eta_1)].$$

Moreover, simple analysis shows that

$$\begin{aligned}\mathrm{Tr}[\mathcal{B}(\eta_1)\mathcal{B}(\eta_2)\cdots\mathcal{B}(\eta_{2n+1})]&=0,\\ \mathrm{Tr}[\mathcal{B}(\eta_1)\mathcal{B}(\eta_2)\cdots\mathcal{B}(\eta_{2n})]&=\mathrm{Tr}[\mathcal{N}(\eta_1)\mathcal{N}(\eta_3)\cdots\mathcal{N}(\eta_{2n-1}) +\mathcal{N}(\eta_2)\mathcal{N}(\eta_4)\cdots\mathcal{N}(\eta_{2n})],\end{aligned} \tag{A4}$$

where matrix $\mathcal{N}(\eta)$ is introduced in Eq. (9). One can see from expressions (A4) that in the formulas (A2) elements of the sums corresponding to odd values of k are zero, whereas elements corresponding to even values of k coincide, since $(-1)^{2n}=1$. Thus one can readily conclude that $\mathrm{Tr}[\mathcal{J}(\eta,\eta')]=\mathrm{Tr}[\mathcal{J}^{-1}(\eta,\eta')]$ for arbitrary η and η'.

APPENDIX B

In this appendix we present the whole system of eight equations whose compatibility condition is Eq. (16). The first four are given by Newton's formulas (15):

$$\begin{aligned}p_1&=-T_1,\\ p_2&=-\tfrac{1}{2}(T_1p_1+T_2),\\ p_3&=-\tfrac{1}{3}(T_1p_2+T_2p_1+T_3),\\ p_4&=-\tfrac{1}{4}(T_1p_3+T_2p_2+T_3p_1+T_4).\end{aligned} \tag{B1}$$

Next four equations are obtained by multiplication of equation $D(\mathcal{P})=\mathcal{O}$ by $\mathcal{P}^{-k}$, calculation of traces of resulting matrix equations, and using properties $T_k=T_{-k}$:

$$\begin{aligned}T_3+p_1T_2+p_2T_1+4p_3+p_4T_1&=0,\\ T_2+p_1T_1+4p_2+p_3T_1+p_4T_2&=0,\\ T_1+4p_1+p_2T_1+p_3T_2+p_4T_3&=0,\\ 4+p_1T_1+p_2T_2+p_3T_3+p_4T_4&=0.\end{aligned} \tag{B2}$$

The compatibility conditions for these two systems of equations are given by Eq. (16).

[1] M. G. Vakhitov and A. A. Kolokolov, Sov. Radiophys. **16**, 783 (1973).
[2] D. J. Mitchell and A. W. Snyder, J. Opt. Soc. Am. B **10**, 1572 (1993).
[3] N. N. Akhmediev and N. V. Ostrovskaya, Sov. Phys. Tech. Phys. **33**, 1333 (1988).
[4] J. Miranda, D. R. Andersen, and S. R. Skinner, Phys. Rev. A **46**, 5999 (1992).
[5] H. T. Tran, J. D. Mitchell, N. N. Akhmediev, and A. Ankiewicz, Opt. Commun. **93**, 227 (1992).
[6] D. R. Andersen and S. R. Skinner, J. Opt. Soc. Am. B **8**, 2265 (1991).
[7] H. T. Tran, J. Opt. Soc. Am. B **11**, 789 (1994).
[8] A. W. Snyder, D. J. Mitchell, and A. Buryak, J. Opt. Soc. Am. B **13**, 1146 (1996).
[9] V. A. Aleshkevich, Y. V. Kartashov, A. A. Egorov, and V. A. Vysloukh, Phys. Rev. E **64**, 056610 (2001).
[10] V. A. Aleshkevich, V. A. Vysloukh, A. A. Egorov, and Y. V. Kartashov, Quantum Electron. **31**, 713 (2001).
[11] J. M. Soto-Crespo and N. Akhmediev, Phys. Rev. E **48**, 4710 (1993).
[12] G. Cohen, Phys. Rev. E **52**, 5565 (1995).
[13] J. M. Soto-Crespo, N. Akhmediev, and A. Ankiewicz, Phys. Rev. E **51**, 3547 (1995).
[14] N. N. Akhmediev, A. V. Buryak, J. M. Soto-Crespo, and D. R. Andersen, J. Opt. Soc. Am. B **12**, 434 (1995).
[15] Y. Chen, Phys. Rev. E **57**, 3542 (1998).
[16] D. C. Hutchings and J. M. Arnold, J. Opt. Soc. Am. B **16**, 513

(1999).
[17] L. Torner, D. Mihalache, D. Mazilu, and N. N. Akhmediev, Opt. Lett. **20**, 2183 (1995).
[18] D. E. Pelinovsky and Y. S. Kivshar, Phys. Rev. E **62**, 8668 (2000).
[19] D. Mihalache, D. Mazilu, and L. Torner, Phys. Rev. Lett. **81**, 4353 (1998).
[20] D. Mihalache, D. Mazilu, and L.-C. Crasovan, Phys. Rev. E **60**, 7504 (1999).
[21] A. V. Buryak and Y. S. Kivshar, Phys. Rev. Lett. **78**, 3286 (1997).
[22] L. Torner, D. Mihalache, D. Mazilu, M. C. Santos, and N. N. Akhmediev, J. Opt. Soc. Am. B **15**, 1476 (1998); D. Mihalache, D. Mazilu, L.-C. Crasovan, and L. Torner, Phys. Rev. E **56**, R6294 (1997).
[23] I. V. Barashenkov, Phys. Rev. Lett. **77**, 1193 (1996); I. V. Barashenkov, D. E. Pelinovsky, and V. E. Zemlyanaya, *ibid.* **80**, 5117 (1998).
[24] V. M. Petnikova, V. V. Shuvalov, and V. A. Vysloukh, Phys. Rev. E **60**, 1 (1999).
[25] F. T. Hioe, Phys. Rev. Lett. **82**, 1152 (1999).
[26] L. D. Carr, C. W. Clark, and W. P. Reinhardt, Phys. Rev. A **62**, 063610 (2000).
[27] L. D. Carr, C. W. Clark, and W. P. Reinhardt, Phys. Rev. A **62**, 063611 (2000).
[28] V. Aleshkevich, V. Vysloukh, and Y. Kartashov, Opt. Commun. **173**, 277 (2000).
[29] V. A. Aleshkevich, V. A. Vysloukh, and Y. V. Kartashov, Quantum Electron. **31**, 257 (2001).
[30] N. Korneev, A. Apolinar-Iribe, V. A. Vysloukh, and M. A. Basurto-Pensado, Opt. Commun. **197**, 209 (2001).
[31] V. Aleshkevich, Y. Kartashov, and V. Vysloukh, J. Opt. Soc. Am. B **18**, 1127 (2001).
[32] V. Aleshkevich, Y. Kartashov, and V. Vysloukh, Opt. Commun. **185**, 305 (2000).
[33] V. Aleshkevich, Y. Kartashov, and V. Vysloukh, Opt. Commun. **190**, 373 (2001).
[34] V. A. Aleshkevich, V. A. Vysloukh, and Y. V. Kartashov, Quantum Electron. **31**, 327 (2001).
[35] L. D. Carr, J. N. Kutz, and W. P. Reinhardt, Phys. Rev. E **63**, 066604 (2001).
[36] L. Berge, T. J. Alexander, and Y. S. Kivshar, Phys. Rev. A **62**, 023607 (2000).
[37] Y. S. Kivshar, Phys. Rep. **298**, 81 (1998).
[38] A. Ankiewicz, W. Krolikowski, and N. N. Akhmediev, Phys. Rev. E **59**, 6079 (1999).
[39] V. E. Zakharov, Sov. Phys. JETP **26**, 994 (1968).
[40] E. Infeld and G. Rowlands, Z. Phys. B **37**, 280 (1980).
[41] V. P. Pavlenko and V. I. Petviashvili, JETP Lett. **26**, 200 (1977).
[42] V. P. Kudashev and A. B. Mikhailovsky, Sov. Phys. JETP **63**, 972 (1986).
[43] E. Infeld and T. Lenkowska-Czerwinska, Phys. Rev. E **55**, 6101 (1997).
[44] V. E. Zakharov and A. M. Rubenchik, Sov. Phys. JETP **38**, 494 (1974).
[45] E. A. Kuznetsov, A. M. Rubenchik, and V. E. Zakharov, Phys. Rep. **142**, 103 (1986).
[46] Y. S. Kivshar and D. E. Pelinovsky, Phys. Rep. **331**, 117 (2000).